STOCHASTIC OPTIMAL DESIGN OF A RURAL MICROGRID

GÜLFEM ER

JULY 2022

STOCHASTIC OPTIMAL DESIGN OF A RURAL MICROGRID

A THESIS SUBMITTED TO THE

GRADUATE SCHOOL

OF

BAHÇEŞEHİR UNIVERSITY

GÜLFEM ER

IN PARTIAL FULFILLMENT OF THE REQUIREMENTS

FOR

THE DEGREE OF

MASTER'S IN INDUSTRIAL ENGINEERING

JULY 2022

T.C.

BAHCESEHIR UNIVERSITY

GRADUATE SCHOOL

MASTER THESIS APPROVAL FORM

Program Name:	Industrial Engineering
Student's Name and Surname:	Gülfem ER
Name Of The Thesis:	Stochastic Optimal Design of a Rural Microgrid
Thesis Defense Date:	01/07/2022

This thesis has been approved by the Graduate School which has fulfilled the necessary conditions as Master thesis.

Prof. Dr. Ahmet ÖNCÜ

Institute Director

This thesis was read by us, quality and content as a Master's thesis has been seen and accepted as sufficient.

	Title/Name	Signature
Thesis Advisor's	Assoc. Prof. Dr. Ethem Çanakoğlu	
Member's	Assist. Prof. Dr. Adnan Çorum	
Member's	Assoc. Prof. Dr. Mehtap Dursun Karahüseyin	

I hereby declare that all information in this document has been obtained and presented in accordance with academic rules and ethical conduct. I also declare that, as required by these rules and conduct, I have fully cited and referenced all material and results that are not original to this work.

Name, Last Name: Gülfem Er

Signature:

ABSTRACT

STOCHASTIC OPTIMAL DESIGN OF A RURAL MICROGRID

Er, Gülfem
Master's Program in Industrial Engineering
Supervisor: Assoc. Prof. Dr. Ethem Çanakoğlu

July 2022, 34 pages

In this thesis, the optimal sizing of a rural microgrid is done by applying two-stage stochastic programming. The system components are a photovoltaic panel, wind turbine, battery, electric vehicles, and hydrogen-based storage. Hydrogen-based storage is composed of an electrolyzer, a hydrogen tank, and a fuel cell. A multi-objective optimization problem with two objectives is solved where the objective functions are life cycle cost minimization and maximization of the system reliability. In order to reflect reliability, an index called loss of power supply probability is used. The problem is solved with mixed-integer linear programming. An hourly real-world data for a one-year period is used for simulations. The uncertainties coming from renewable resources, demand, and electric vehicle users are considered during system design. Different cases are created to see the effect of electric vehicles and hydrogen storage in capacity configuration. Even though hydrogen storage is an expensive storage type when compared with a battery, it is more environmentally friendly. Because of this reason, the usage of hydrogen storage may increase in the future.

Key Words: Microgrid, Uncertainty, Stochastic Optimization, Electric Vehicles, Hydrogen Storage

ÖZ

KIRSAL BİR MİKRO ŞEBEKENİN STOKASTİK OPTİMAL TASARIMI

Er, Gülfem
Endüstri Mühendisliği Yüksek Lisans Programı
Tez Danışmanı: Doç Dr. Ethem Çanakoğlu

Temmuz 2022, 34 sayfa

Bu tezde, bir kırsal mikro şebekenin optimal boyutlandırılması, iki aşamalı stokastik programlama uygulanarak yapılır. Sistem bileşenleri bir fotovoltaik panel, rüzgar türbini, pil, elektrikli araçlar ve hidrojen bazlı depolamadır. Hidrojen bazlı depolama, bir elektrolizör, bir hidrojen tankı ve bir yakıt hücresinden oluşur. Amaç fonksiyonlarının yaşam döngüsü maliyeti minimizasyonu ve sistem güvenilirliğinin maksimizasyonu olduğu iki amacı olan çok amaçlı bir optimizasyon problemi çözülmüştür. Güvenilirliği yansıtmak için güç kaynağı kaybı olasılığı adı verilen bir endeks kullanılır. Problem karışık tamsayılı doğrusal programlama ile çözülmüştür. Simülasyonlar için bir yıllık bir dönem için saatlik gerçek dünya verileri kullanılır. Sistem tasarımı sırasında yenilenebilir kaynaklardan, talepten ve elektrikli araç kullanıcılarından kaynaklanan belirsizlikler göz önünde bulundurulur. Kapasite konfigürasyonunda elektrikli araçlar ve hidrojen depolamanın etkisini görmek için farklı durumlar oluşturulmuştur. Hidrojen depolama, pille karşılaştırıldığında pahalı bir depolama türü olsa da daha çevrecidir. Bu nedenle gelecekte hidrojen depolama kullanımı artabilir.

Anahtar Kelimeler: Mikro şebeke, Belirsizlik, Stokastik Optimizasyon, Elektrikli Araçlar, Hidrojen Depolama

Dedicating

ACKNOWLEDGEMENTS

I wish to express my deepest gratitude to my supervisor Assoc. Prof. Dr. Ethem ÇANAKOĞLU for his guidance, advice, criticism, encouragement, and insight throughout the research.

I would also like to thank my parents, Sevinç ER and Kartal ER, and my brother Egemen ER for their great support. Without their understanding, and continuous support, I could have never been able to aspire for this level of education and complete this study.

TABLE OF CONTENTS

LIST OF TABLES

TABLES

LIST OF FIGURES

FIGURES

LIST OF ABBREVIATIONS

COE	Cost of Energy
ENS	Energy Not Supplied
EV	Electric Vehicle
GA	Genetic Algorithm
IP	Integer Programming
LCC	Life Cycle Cost
LCOE	Levelized Cost of Energy
LOLP	Loss of Load Probability
LP	Linear Programming
LPSP	Loss of Power Supply Probability
MC	Monte Carlo
MILP	Mixed Integer Linear Programming
MOGA	Multi-objective Genetic Algorithm
MOPSO	Multi-objective Particle Swarm Optimization
NPC	Net Present Cost
NSGA-II	Non-dominated Sorting Genetic Algorithm II
PEM	Polymer Electrolyte Membrane
PSO	Particle Swarm Optimization
SA	Simulated Annealing
SAIDI	System Average Interruption Duration Index
SAIFI	System Average Frequency Duration Index
SOC	State of Charge

LIST OF SYMBOLS

Area of a PV panel	A_{PV}
Available construction area for the microgrid system	A_{MG}
Battery charging efficiency	n_{Bat}^{-}
Battery charging power flow	$P_{Bat}^{-}(t,s)$
Battery discharging efficiency	n_{Bat}^{+}
Battery discharging power flow	P_{Bat}^{+}(t,s)
Capacity of a battery	E_{Bat}
Capacity of an EV	$E_{EV,c}$
Capacity of the electrolyzer	N_{El}
Capacity of the fuel cell	N_{Fc}
Capacity of the hydrogen tank	N_{Ht}
Deficit power	$Dp(t,s)$
Electrolyzer efficiency	η_{El}
Epsilon	ε
EV charging efficiency	n_{EV}^{-}
EV charging power flow	$P_{EV}^{-}(t,s,c)$
EV discharging efficiency	n_{EV}^{+}
EV discharging power flow	$P_{EV}^{+}(t,s,c)$
Fuel cell efficiency	η_{Fc}
Hydrogen tank efficiency	η_{Ht}
Input power from renewables to the electrolyzer	$P_{Wtpv-El}(t,s)$
Number of batteries	N_{Bat}
Number of PV panels	N_{PV}

Number of wind turbines	N_{WT}
Output power of a single PV panel	$p_{pv}(t,s)$
Output power of a single wind turbine	$p_{wt}(t,s)$
Output power of the fuel cell	$P_{Fc}(t,s)$
Power delivered from hydrogen tank to the fuel cell	$P_{Ht-Fc}(t,s)$
Power supplied from electrolyzer to the hydrogen tank	$P_{El-Ht}(t,s)$
PV efficiency	η_{PV}
Solar irradiance	$R(t,s)$
Surplus power	$Sp(t,s)$
Total energy of an EV	$T_{EV}(t,s,c)$
Total energy of the batteries	$T_{Bat}(t,s)$
Total energy stored in the hydrogen tank	$T_{Ht}(t,s)$
Total output power of PV panels	$P_{PV}(t,s)$
Total output power of wind turbines	$P_{WT}(t,s)$

Chapter 1

Introduction

Energy is crucial to the community to sustain their life with desired quality. There are diverse types of energy sources to fulfill this demand. These resources are divided into two separate groups: renewable energy sources and nonrenewable energy sources. The usage of renewable resources is increasing day by day since it supplies clean energy with lower costs (Bull et al., 2001, pp. 1216-1226). There are various renewable sources such as wind energy, solar energy, biomass, hydropower, and geothermal. Between these sources, hydropower is the most used renewable energy source in the world. The second most used is wind energy and solar power follows it.

Recently, these renewable sources are taking part in isolated systems such as microgrid systems. A typical microgrid system is composed of renewables such as wind and solar energy. Traditional energy resources are still used in these systems but because of the benefits of renewables, usage of them is more common. In consequence of the intermittent nature of renewables, storage systems are generally preferred in microgrid systems. A storage system has two roles. One of them is storing the surplus energy generated. Another one is, supplying energy to the system if the generation from the renewables is not enough to meet the demand. There are various advantages offered by microgrid systems (Hartono et al., 2013, pp. 127-132). It provides higher power quality and because of the renewables, it is environmentally friendly. Microgrid systems are preferred as an alternative solution for rural areas without access to energy. These systems can also be used as grid-connected. In this case, they can supply energy to the grid, oppositely can take energy from the grid if the generation is not sufficient.

The optimal sizing of microgrid systems is an important point to install and manage the system without or with the minimum number of problems. In each optimization model, there should be an objective function, constraints, and input parameters. There are various objectives that can be studied in microgrid systems such as minimization of the cost, emission, and maximization of reliability. Similarly, there are multiple constraints that depend on the components and system conditions. In addition to this, there are parameters related to each component and the system in general. If the system contains renewable sources, one of the input parameters will be weather conditions such as solar irradiance and wind speed. These parameters can be the real data if the location of the system is determined. If the measurement is not possible, the historical data can be used.

The details of these objectives, constraints, and parameters will be explained in the following sections.

1.1 Optimization in Microgrid Systems

In the optimization of microgrid systems, there are various techniques (Fathima et al., 2015, pp. 431–446). These techniques can be examined mainly in two groups: mathematical programming, and meta-heuristic methods. While mathematical optimization provides an optimal solution, meta-heuristic methods do not guarantee optimality. In mathematical optimization techniques some of the well-known ones are Integer Programming (IP), Linear Programming (LP), and Mixed Integer Linear Programming (MILP). Also, there are diverse meta-heuristic methods such as Particle Swarm Optimization (PSO), Genetic Algorithm (GA), and Simulated Annealing (SA). In some cases, it is almost impossible to find the optimal solution. For instance, it might take too much time to reach the optimal result in big sized problems. In this situation meta-heuristic methods can be preferred. Otherwise, mathematical methods ensure more accurate results since they provide optimality.

In a typical optimization problem, there should be an objective function, constraints, and parameters. In some cases, there can be more than one objective function. If there is one objective function it is called a single objective, if there are two or more objective functions, it is called multi-objective optimization. During optimal sizing of a microgrid system, there are various objectives that can be studied. The most widely used objectives are cost and emission minimization, reliability maximization and if the system is grid-connected network loss can be examined. In addition, emission minimization can be studied if there is an energy source which is nonrenewable such as diesel generators. Renewable sources do not cause carbon emissions because of that this objective function becomes useless if the system consists of renewables.

The cost minimization can be divided into diverse groups since there are different types of costs in a microgrid system. The most popular three cost types are Levelized cost of energy (LCOE), Net present cost (NPC), and Life cycle cost (LCC). NPC is the present value of all the costs of setting and operating the components over the project life span. LCOE is the price per unit of energy. LCC is the summation of the net present value of each component in the system.

Another important objective function is the reliability function. There are different indexes that measure the reliability of the system. Some of those indexes are SAIFI, SAIDI, ENS, LOLP, and LPSP (Abdulgalil et al., 2018), (Gazijahani et al., 2018), (Jacob et al., 2021). SAIFI calculates the average number of failures per customer, SAIDI is used to find the total duration of the failures per customer and ENS gives the total energy which is not supplied to the customer. LOLP and LPSP are probability indexes. LOLP is the probability of not meeting the demand and LPSP is the probability of power supply loss. Between these indexes the most widely used one is LPSP.

In the optimal installation of a microgrid system with renewable resources, stochastic optimization techniques become essential as a result of uncertainties that occur from renewable resources such as solar and wind. There are various solution methods, most preferred ones are chance-constrained optimization, two-stage stochastic optimization, and robust optimization. The difference between robust and two-stage stochastic optimization is while robust optimization considers the worst scenario, two-stage stochastic optimization solves with respect to average values of the scenarios. Another useful method is Monte Carlo (MC) simulations, by estimating the distribution of the data sets, and helps solve the problem. Similar scenarios are eliminated with this technique.

1.2 Literature Review

In the literature, there are studies that deal with the stochastic optimal design of microgrid systems by considering uncertainties in the system. These studies can be divided into two main groups isolated and grid-connected microgrid systems. In (Lazaroiu et al., 2016, pp. 1-5), a grid-connected microgrid system with PV, thermal engine, and the battery is designed. Both deterministic and stochastic optimization is applied during modelling. The objective function is operational cost minimization. The uncertainty of solar generation is considered. In (Gazijahani et al., 2018, pp. 999-1015), robust optimization is applied by considering uncertainties from market price, wind, and solar. A grid-connected microgrid system is designed with an investment cost minimization objective. Reliability is taken as a constraint in the optimization problem. In (Nazari et al., 2019, pp. 281-294), optimal sizing of the storage system is done for a grid-connected microgrid system. Different types of storages are compared such as battery, flywheel, and pumped hydro. The two-stage stochastic optimization model is applied to minimize the total yearly cost. The market price is taken as an uncertain parameter. Uncertainties of solar, wind, and demand are considered as constraints during modelling.

There are also studies for stochastic optimal design in isolated microgrids which are not connected to the grid. These studies can be grouped according to their solution technique: heuristic, meta-heuristic, and mathematical methods. In (Bashir et al., 2012, pp. 1081-1086), a microgrid system consisting of wind, PV, and battery is modelled while minimizing NPC. As a solution method, modified PSO is proposed. MC is applied during uncertainty modelling of renewables. In another study, (Guo et al., 2014, pp. 1263-1273), a multi-objective optimization is done with two objectives where objectives are NPC and emission minimization. System components are wind turbine, PV, diesel generator, and battery. During optimization, the NSGA-II algorithm and chance-constrained programming are applied. Uncertainties from renewables and demand are considered in system design. A PV, wind turbine and diesel based microgrid system is modelled in (Maheri et al., 2014, pp. 650-661). Multi-objective optimization is applied by minimizing LCOE and maximizing the reliability of the system. GA is used for optimal sizing and MC simulations are applied for uncertainty modelling of renewable sources and demand. In (Kamjoo et al., 2016, pp. 187-194), a microgrid system with wind, PV, and battery is designed. Multi-objective problem is solved by chance-constrained programming and NSGA-II. Objectives are total cost minimization and reliability maximization of. MC simulations are utilized for uncertainty modelling of renewable generation. Another multi-objective study is done in (Sadeghi et al., 2020, pp. 118471) where the objectives are LCC minimization and reliability maximization. A microgrid system that consists of PV, wind turbine, battery, and EV is modelled by PSO. Uncertainties coming from EV are modelled by using MC simulations. An isolated microgrid system is modelled by using stochastic and deterministic optimization in (Haidar et al., 2020, pp. 102391). A combination of MOPSO and regression methods is presented for stochastic optimization. COE and NPC are cost objectives and uncertainty of renewable generation is considered as another objective function. The system components are PV, hydro turbine, diesel generation, and battery. Uncertainties from demand and renewables are considered during optimal sizing. In (Gamil et al., 2021, pp. 483-515), a multi-objective optimization is done by minimizing the total system cost and loss of power supply. The components of the microgrid system are biomass generator, wind, PV, and battery. MOGA is applied during system optimization and in order to reflect uncertainties of renewables MC simulations are used.

There are also studies that applied mathematical optimization methods such as MILP, etc. for optimal sizing of rural microgrid systems. In (Arun et al., 2009, pp. 1013-1025), a PV-battery-based microgrid design is studied. Chance-constrained programming is used for optimization by minimizing COE. Uncertainty modelling of solar generation is done by using MC simulations. In (Narayan et al., 2017, pp. 399-408), an isolated microgrid system consisting of wind turbine, PV, diesel generator, and the battery is modelled. Markovitz objective function is introduced to minimize investment risks that occur from uncertainties. Two-stage stochastic optimization is utilized by considering uncertainties from renewables and demand. Similarly, in (Balderrama et al., 2019, pp. 116073), the two-stage stochastic optimization model is solved by using MILP. A rural microgrid system is modelled which consists of wind, PV, diesel, micro-hydro, and battery. The objective function is the minimization of NPC and uncertainties from demand and solar generation are considered the optimization model. Also, in (Stevanato et al., 2020, pp. 16-29) the objective function is NPC minimization. A PV-wind-diesel-battery-based isolated microgrid system is designed. Two-stage stochastic optimization is applied, and the problem is solved by

MILP. In system sizing, only uncertainties arising from demand are taken into account. In (Naderi et al., 2022, pp. 54-65), optimal sizing of a rural microgrid is studied with capital, operation, and maintenance cost minimization objective function. MILP is used to solve the optimization problem, in order to generate uncertainties MC simulations are utilized.

In this thesis, the optimal sizing of a rural microgrid is studied by using two-stage stochastic optimization. A multi-objective problem is solved by MILP where the objectives are maximization of LCC and minimization of LPSP. The system consists of PV, wind turbine, battery, hydrogen storage (electrolyzer, hydrogen tank, fuel cell), and EV. During system design, uncertainties of demand, renewables, and EV user behaviors are considered. System simulations are made by using real-world data for 365 days with hourly data sets. The comparison of the rural microgrid designs in the literature is presented in Table 1.

Table 1: Comparison between presented rural microgrid systems.

	PV	Wind	Others	Storage	Objective	Uncertain Parameters	Method
(Bashir et al., 2012)	✓	✓		Battery	NPC	Solar, wind	Metaheuristic
(Guo et al., 2014,)	✓	✓	Diesel	Battery	NPC and emission	Solar, wind, demand	Metaheuristic
(Maheri et al., 2014)	✓	✓	Diesel	Battery	LCOE and reliability	Solar, wind, demand	Metaheuristic
(Kamjoo et al., 2016)	✓	✓		Battery	Total cost and reliability	Solar, wind	Metaheuristic
(Sadeghi et al., 2020)	✓	✓	EV	Battery	LCC and reliability	EV	Metaheuristic
(Haidar et al., 2020)	✓		Hydro turbine, diesel	Battery	COE/NPC and uncertainty of renewables	Solar, wind, demand	Metaheuristic
(Gamil et al., 2021)	✓	✓	Biomass generator		Total cost and LPSP	Solar, wind	Metaheuristic
(Arun et al., 2009)	✓			Battery	COE	Solar	Mathematical
(Narayan et al., 2017)	✓	✓	Diesel	Battery	Investment risk	Solar, wind, demand	Mathematical
(Balderrama et al., 2019)	✓	✓	Micro hydro, diesel	Battery	NPC	Solar, demand	Mathematical
(Stevanato et al., 2020)	✓	✓	Diesel	Battery	NPC	Demand	Mathematical
(Naderi et al., 2022)	✓	✓		Battery	Capital,operating and maintenance cost	Solar, wind	Mathematical
This paper	✓	✓	EV	Battery, Hydrogen storage	LCC and reliability	Solar, wind, demand, EV	Mathematical

Chapter 2

System Modelling

In this thesis, the optimal sizing of a rural microgrid system is presented. The system consists of a wind turbine, PV, battery, hydrogen storage, and EV. The number of wind turbines, PV panels, batteries, and the capacity of electrolyzer, hydrogen tank, and fuel cell are the decision variables whereas the number of EVs is constant which equals 10. The schematic representation of the model is shown in Figure 2.1. The modelling of each component is explained in this section.

Figure 1. Rural microgrid system.

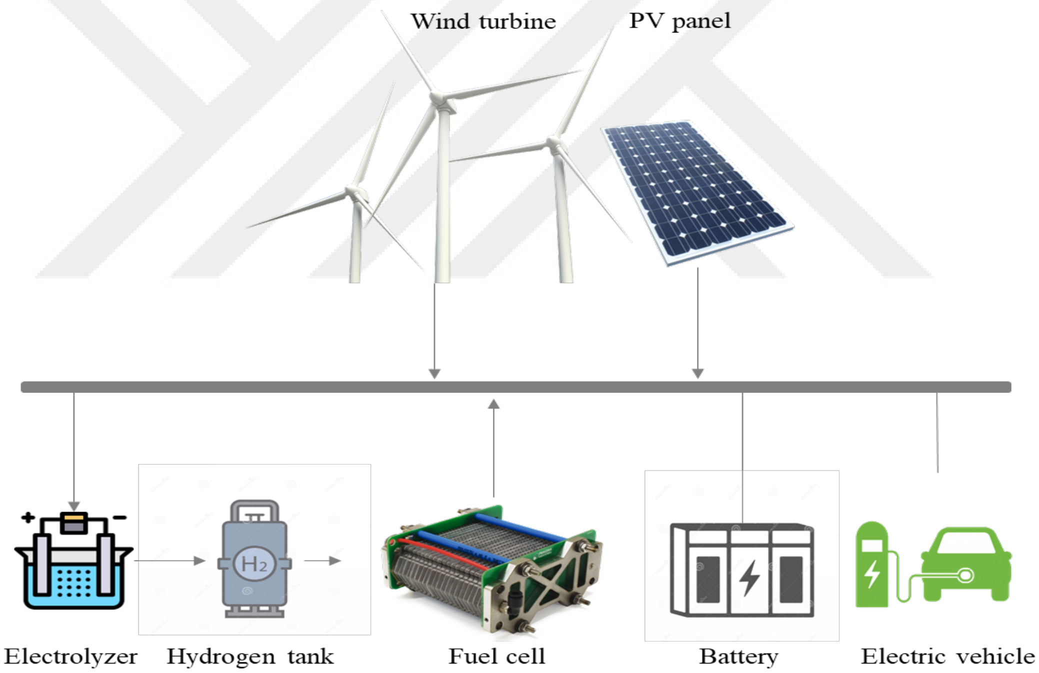

2.1 Wind Modelling

The generated power from a wind turbine for each scenario s can be calculated as:

$$p_{wt}(t,s) = \begin{cases} 0 & v(t,s) \leq v_{cut-in} \ or \ v(t,s) \geq v_{cut-out} \\ P_r \dfrac{v(t,s)^k - v_{cut-in}{}^k}{v_r{}^k - v_{cut-in}{}^k} & v_{cut-in} < v(t,s) < v_r \\ P_r & v_r < v(t,s) < v_{cut-out} \end{cases} \quad \mathbf{(2.1)}$$

In (2.1), $v(t)$ represents the wind speed at time t, v_{cut-in} and $v_{cut-out}$ represent cut-in and cut-out wind speeds where the wind turbine stop working. v_r is defined as rated wind speed and k represents the Weibull shape parameter. The total output of all wind turbines in the microgrid system can be calculated as:

$$P_{WT}(t,s) = N_{WT} \times p_{wt}(t,s) \quad \mathbf{(2.2)}$$

where N_{WT} is the total number of wind turbines in the system.

2.2 PV Modelling

The generated power from a single PV panel can be calculated as:

$$p_{pv} = R(t,s) \times A_{PV} \times \eta_{PV} \quad \mathbf{(2.3)}$$

where $R(t,s)$ represents solar radiation (W/m^2) of the area where the microgrid system will be constructed at time t. A_{PV} is the area (m^2) of a PV panel and η_{PV} is the efficiency of a PV panel. The total output of all PV panels in the microgrid system can be calculated as:

$$P_{PV}(t) = N_{PV} \times p_{PV}(t,s) \quad \mathbf{(2.4)}$$

where N_{PV} is the total number of PV panels in the system.

2.3 Battery Modelling

In this microgrid system, one of the storage devices is selected as a Li-ion battery. The power equation for batteries at time t for each scenario s can be formulated as:

$$(-P_{Bat}^{+}(t,s) \times \Delta t / n_{bat}^{+}) + T_{Bat}(t,s) + (P_{Bat}^{-}(t,s) \times \Delta t \times n_{bat}^{-}) = T_{Bat}(t+1,s) \qquad \mathbf{(2.5)}$$

where $P_{Bat}^{-}(t,s)$ and $P_{Bat}^{+}(t,s)$ is the charge and discharge power flow of batteries (W), n_{bat}^{-} and n_{bat}^{+} are battery charge-discharge efficiencies, $T_{Bat}(t,s)$ represents the total energy of the batteries in the system and Δt is the time interval which is equal to 1 hour in this model. The maximum and minimum charge & discharge capacity of batteries will be defined through the state of charge (SOC) of the batteries which defines the battery charge level. SOC value of a battery can be calculated as:

$$SOC_{Bat}(t,s) = \frac{T_{Bat}(t,s)}{E_{Bat} \times N_{Bat}}. \qquad \mathbf{(2.6)}$$

E_{Bat} represents the maximum capacity of each battery (Wh), and N_{Bat} represents the total number of batteries in the microgrid system.

2.4 Hydrogen-based Storage Modelling

Hydrogen-based storage is utilized in this thesis which consists of a PEM electrolyzer, a hydrogen tank, and a PEM fuel cell. The power equations are obtained from (Mohseni et al., 2020, pp. 114224) and (Moghaddam et al., 2019, pp. 1412-1434).

2.4.1 Electrolyzer

An electrolyzer is used to generate hydrogen and oxygen by decomposing the water with the help of an electrical current. The power supplied from the electrolyzer to the hydrogen tank can be calculated as:

$$P_{El-Ht}(t,s) = P_{Wtpv-El}(t,s) \times n_{El} \qquad (2.7)$$

where $P_{El-Ht}(t,s)$ is the power supplied from the electrolyzer to the hydrogen tank, $P_{Wtpv-El}(t,s)$ is the input power from renewables to the electrolyzer and n_{El} is the efficiency of the electrolyzer.

2.4.2 Hydrogen Tank

A hydrogen tank is used to store hydrogen that is generated from the electrolyzer. The total energy stored in a hydrogen tank is shown in the power equation below:

$$(P_{El-Ht}(t,s) \times \Delta t) + T_{Ht}(t,s) - (P_{Ht-Fc}(t,s) \times \Delta t \times n_{Ht}) = T_{Ht}(t+1,s). \qquad (2.8)$$

$T_{Ht}(t,s)$ and $T_{Ht}(t+1,s)$ represent the total energy stored in the tank at time t and $t+1$ respectively. $P_{Ht-Fc}(t,s)$ is the power delivered from the hydrogen tank to the fuel cell and n_{Ht} represents the efficiency of the hydrogen tank. The mass (kg) of the hydrogen stored in the tank at time t can be calculated as:

$$m_{Ht}(t,s) = \frac{T_{Ht}(t,s)}{HHV_{H2}} \qquad (2.9)$$

where HHV_{H2} is the higher heating value of the hydrogen which has a constant value of 39.7 kWh.

2.4.3 Fuel Cell

A fuel cell is used to convert chemical energy to electrical energy. The output power of the fuel cell is calculated as:

$$P_{Fc}(t,s) = P_{Ht-Fc}(t,s) * n_{Fc}. \qquad (2.10)$$

n_{Fc} represents the efficiency of the fuel cell.

2.5 EV Modelling

In this study, electrical vehicles are used as backup batteries which are charged and discharged by connecting to the system. The power equation of EVs is similar to the batteries but cannot be aggregated since all cars will not be available at each time interval. Because of this reason, the power equation of each car with c index can be shown as follows:

$$(-P_{EV}^{+}(t,s,c) \times \Delta t / n_{EV}^{+}) + T_{EV}(t,s,c) + (P_{EV}^{-}(t,s,c) \times \Delta t \times n_{EV}^{-}) = T_{EV}(t+1,s,c) \quad \mathbf{(2.11)}$$

$P_{EV}^{-}(t,s,c)$ and $P_{EV}^{+}(t,s,c)$ represent EV charge & discharge power flows respectively, n_{EV}^{-} and n_{EV}^{+} EV battery charge & discharge efficiencies and $T_{EV}(t,s,c)$ is the total energy (Wh) stored in each EV. Similar to the batteries SOC of EVs can be calculated as follows:

$$SOC_{EV}(t,s,c) = \frac{T_{EV}(t,s,c)}{E_{EV,c}} \ . \quad \mathbf{(2.12)}$$

$E_{EV,c}$ represents the maximum capacity of each car c.

Chapter 3

Stochastic Programming

In this section, the multi-objective optimization technique will be introduced, and the stochastic optimization method will be defined.

3.1 Multi-Objective Optimization

In this thesis, a multi-objective optimization method is applied for problem-solving. The goal of the model is to find the optimum number of components in the system. The number of wind turbines, PV panels, batteries, the capacity of electrolyzer, fuel cell in W, and the capacity of the fuel tank in kg are the decision variables. However, the number of EVs is constant which is equal to 10 in this model. There are two objective functions in the model, one of them is the minimization of the LCC and the other objective is the minimization of LPSP. In the literature, there are various multi-objective optimization techniques such as the weighted sum method, global criterion approach, and ε-constraint method (Marler 2005). In this study, the ε-constraint method is applied where one objective is converted to a constraint and the other one remains as the objective function (Shadkam et al., 2015). The mathematical formulation of the method for a minimization problem can be shown as follows:

$$min\ OF_1(x), \tag{3.1}$$

$$s.t. \quad OF_2(x) \leq b, \tag{3.2}$$

$$x \in X, \tag{3.3}$$

where $OF_1(x)$ and $OF_2(x)$ are the objective functions and b represents the budget for the ε-constraint. In this model, LCC minimization remains as the objective function and LPSP is taken as the ε-constraint. During optimization, different values of LPSP will be studied and for each LPSP value, the total LCC will be calculated.

3.2 Two-Stage Stochastic Optimization

In this thesis, to handle the uncertainties from renewables and the demand two-stage stochastic optimization is applied. The data sets used are hourly data sets for 365 days. Each day is considered as a scenario, therefore a scenario-based model is applied to reflect the uncertainties in the rural microgrid system. In this model, there are two types of decision variables, the first stage variables, and the second stage variables. In the first stage, here-and-now decisions are made which determine the system structure before the uncertainty is disclosed. The number of wind turbines, PV panels, batteries, and the capacity of electrolyzer (W), hydrogen tank (kg), and fuel cell (W) is determined in this stage. Therefore, the capital assigned to the microgrid system will be decided in this stage. On the other hand, there are wait-and-see decisions which are made after the uncertainties are revealed.

In the second stage, there are 365 scenarios that represent 365 days. Each scenario includes the level of solar irradiance, wind speed, EV charge/discharge pattern, and EV arrival/departure time schedule. The second stage variables are EV/battery charge & discharge schedule and the level of deficiency at each time interval which is one hour. In all scenarios, the total deficiency level and corresponding level of LPSP are calculated and for the decision variables the feasible region is determined where LPSP values are always less than or equal to the ε-constraint.

All constraints in the model are assigned as second-stage constraints except the constraint related to the area limitation of the microgrid system which does not depend on the scenarios. The second stage variables will not affect the system cost since the objective function LCC is defined in the first stage. The stochastic scenario structure is shown in Figure 2. It includes the decision variables and input parameters for Stage I and Stage II.

Figure 2. Two-stage stochastic optimization model.

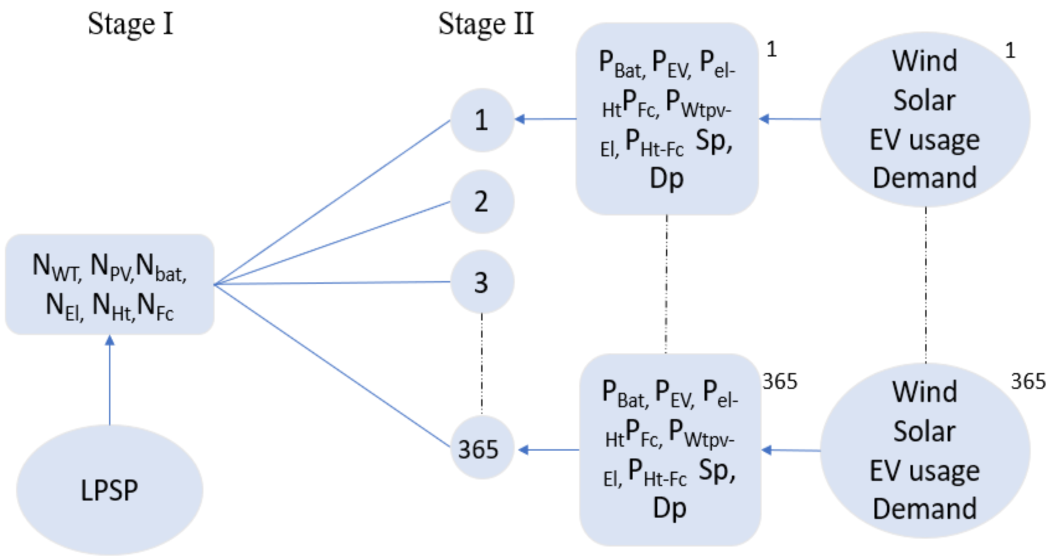

Chapter 4

Problem Formulation

In this section, objective functions, system constraints, and component constraints will be presented.

4.1 Objective Function

The objective function is to minimize the total annualized LCC of the model which includes the capital cost, operation & maintenance cost, and replacement cost of the system components which will not include EVs. The total LCC of the microgrid system can be calculated as follows:

$$min. \sum_{m=PV,WT,Bat,El,Ht,Fc} LCC_m \qquad \textbf{(4.1)}$$

where the life cycle cost is the summation of the capital cost CC, operation & maintenance cost OM, and replacement cost RC.

$$LCC = CC + MC + RC \qquad \textbf{(4.2)}$$

4.1.1 Life cycle cost of Wind Turbine

The total annualized life cycle cost of a wind turbine includes capital cost and operation & maintenance cost. The lifetime of a wind turbine equals the lifetime of the microgrid system, therefore there will not be a replacement cost. The LCC for wind turbines can be calculated as:

$$LCC_{WT} = (CC_{WT} + MC_{WT}) \times N_{WT} \qquad \textbf{(4.3)}$$

The capital cost and operation & maintenance cost of a wind turbine can be defined as follows:

$$CC_{WT} = CRF \times A_{WT} \times C_{WT} \qquad \textbf{(4.4)}$$

$$MC_{WT} = A_{WT} \times C_{Mnt-WT} \quad \mathbf{(4.5)}$$

where A_{WT} represents the swept area of the wind turbine, C_{WT} is the unit cost and C_{Mnt-WT} is the annual operation & maintenance cost of a single wind turbine. CRF is the capital recovery factor that is used to convert present worth to annual cash flows. CRF is expressed as:

$$CRF(i,n) = \frac{i(1+i)^n}{(1+i)^n - 1}\,. \quad \mathbf{(4.6)}$$

i denotes the interest rate and n is the lifetime of the project.

4.1.2 Life cycle cost of PV

The total annualized life cycle cost of a PV panel is calculated similarly to wind turbines which includes capital cost and operation & maintenance cost. The lifetime of a PV panel equals the lifetime of the microgrid system, therefore there will not be a replacement cost. The LCC for PV panels can be expressed as:

$$LCC_{PV} = (CC_{PV} + MC_{PV}) \times N_{PV} \quad \mathbf{(4.7)}$$

The capital cost and operation & maintenance cost of a PV panel can be calculated as follows:

$$CC_{PV} = CRF \times A_{PV} \times C_{PV} \quad \mathbf{(4.8)}$$

$$MC_{PV} = A_{PV} \times C_{Mnt-PV} \quad \mathbf{(4.9)}$$

where A_{PV} represents the surface area of the PV panel, C_{PV} is the unit cost and C_{Mnt-PV} is the annual operation & maintenance cost of a single PV panel.

4.1.3 Life cycle cost of Battery

The annual LCC of batteries includes capital cost, operation & maintenance cost, and also replacement cost since the lifetime of batteries is 5 years for this model the batteries should be replaced every 5 years during the lifetime of the project. The total annualized LCC of batteries can be defined as:

$$LCC_{Bat} = (CC_{Bat} + MC_{Bat}) \times N_{Bat} \qquad (\mathbf{4.10})$$

The capital cost of a battery can be calculated as follows:

$$CC_{Bat} = CRF_{Bat} \times C_{Bat} \qquad (\mathbf{4.11})$$

C_{Bat} is the unit cost of the battery and CRF is defined separately for the battery because of its shorter lifetime than the planning period. As a result, CRF for battery should be expressed as:

$$CRF(i, 5) = \frac{i(1+i)^5}{(1+i)^5 - 1}\,. \qquad (\mathbf{4.12})$$

4.1.4 Life cycle cost of Electrolyzer

Similar to the renewables in the system, there will not be a replacement cost for the electrolyzer since the lifetime is the same as the planning period of the project. There will be capital and operation & maintenance costs. The annualized LCC can be calculated as:

$$LCC_{El} = (CC_{El} + MC_{El}) \times N_{El} \qquad (\mathbf{4.13})$$

where N_{El} represents the capacity of the electrolyzer in $Watt$ and the capital cost of the electrolyzer can be defined as:

$$CC_{El} = CRF \times C_{El}. \tag{4.14}$$

C_{El} denotes the electrolyzer unit cost per $Watt$.

4.1.5 Life cycle cost of Hydrogen tank

The annualized LCC of the hydrogen tank is calculated as in (4.15) which includes only capital cost and operation & maintenance cost. Since the life span of it equals the project lifetime, there will not be any replacement cost.

$$LCC_{Ht} = (CC_{Ht} + MC_{Ht}) \times N_{Ht} \tag{4.15}$$

The capital cost of the hydrogen tank can be expressed as follows:

$$CC_{Ht} = CRF \times C_{Ht} \tag{4.16}$$

where C_{Ht} represents the unit cost of the hydrogen tank per kg.

4.1.6 Life cycle cost of Fuel cell

Similar to the batteries there will be a replacement cost for the fuel cells since the lifetime of it is specified as 5 years. The total annual LCC of the fuel cell can be calculated as:

$$LCC_{Fc} = (CC_{Fc} + MC_{Fc}) \times N_{Fc} \tag{4.17}$$

where N_{Fc} denotes the capacity of the fuel cell in $Watt$.

The capital cost of the fuel cell can be defined as follows:

$$CC_{Fc} = CRF_{Fc} \times C_{Fc}. \tag{4.18}$$

C_{Fc} is the unit cost of the fuel cell per $Watt$. CRF of the fuel cell is calculated from equation (4.12) which was defined for the batteries. Since the lifetime of the batteries and the fuel cells are the same, the CRF calculation for these components will be also the same.

4.2 Reliability Constraint

According to the ε-constraint method, the reliability object is converted to a constraint. As a reliability index, LPSP is utilized. The LPSP constraint for each scenario can be defined as follows:

$$\frac{\sum_{t=1}^{24} Dp(t,s)}{\sum_{t=1}^{24} Pd(t,s)} \leq LPSP. \qquad \textbf{(4.19)}$$

$Dp(t,s)$ denotes the power not supplied also called as deficit power and $Pd(t,s)$ represents the demand at time t and scenario s.

4.3 Component Constraints

In the optimal design of the microgrid system, there are constraints related to system components such as power limitations, capacity limitations, etc. The capacity limitation for the battery and EV is defined through SOC. The mathematical formulation of these limitations are shown as follows:

$$SOC_{min-Bat} \leq SOC_{Bat}(t,s) \leq SOC_{max-Bat} \qquad \textbf{(4.20)}$$

$$SOC_{min-EV} \leq SOC_{EV}(t,s) \leq SOC_{max-EV} \qquad \textbf{(4.21)}$$

where SOC_{min} and SOC_{max} represent the minimum and maximum SOC levels respectively for both batteries and EVs. Since the SOC formula is nonlinear as in (2.6) and (2.12), the capacity limitations will be defined through the total energy levels of the batteries and EVs:

$$E_{Bat} \times N_{Bat} \times SOC_{min-Bat} \leq T_{Bat}(t,s) \leq E_{Bat} \times N_{Bat} \times SOC_{max-Bat} \quad \mathbf{(4.22)}$$

$$E_{EV,c} \times SOC_{min-EV} \leq T_{EV}(t,s,c) \leq E_{EV,c} \times SOC_{max-EV} \quad \mathbf{(4.23)}$$

In addition, there will be a limitation on the instant power flow of the batteries and EVs for both charge and discharge states. These constraints can be expressed as follows:

$$P_{Bat}^{-}(t,s) \leq N_{Bat} \times P_{Bat-max}^{-} \quad \mathbf{(4.24)}$$

$$P_{Bat}^{+}(t,s) \leq N_{Bat} \times P_{Bat-max}^{+} \quad \mathbf{(4.25)}$$

$$P_{EV}^{-}(t,s,c) \leq P_{EV-max}^{-} \quad \mathbf{(4.26)}$$

$$P_{EV}^{+}(t,s,c) \leq P_{EV-max}^{+} \quad \mathbf{(4.27)}$$

where $P_{Bat-max}^{-}(t,s)/P_{EV-max}^{-}(t,s)$ denotes maximum charge capacity of the battery and EV respectively. $P_{Bat-max}^{+}(t,s)/P_{EV-max}^{+}(t,s)$ represents the maximum discharge capacity of the battery and EV respectively. There are also constraints related to the components of the hydrogen storage. The total energy stored in a hydrogen tank should be in a specific range which can be defined as follows:

$$T_{Ht-min} \leq T_{Ht}(t,s) \leq T_{Ht-max} \quad \mathbf{(4.28)}$$

where T_{Ht-min} and T_{Ht-max} represents the minimum and maximum energy stored in a hydrogen tank. The minimum energy is the 5% of T_{Ht-max} which was recommended in (Kaviani et al., 2009, pp. 2380-2390). The total energy stored in the hydrogen tank at the end of the year should be greater than or equal to the level of energy at the beginning of the initial energy level. This condition is shown in (4.29).

$$T_{Ht}(t=0,s=0) \leq T_{Ht}(t=24,s=365) \quad \mathbf{(4.29)}$$

There is a power limitation for the fuel cell and the electrolyzer. The equations are adapted from (Khiareddine et al., 2018, pp. 743-762).

$$P_{Fc}(t,s) \leq \frac{2 \times 96487 \times V_{FC} \times q_{H_2}}{3600 \times 1000} \times N_{Fc} \qquad \mathbf{(4.30)}$$

V_{FC} is the output voltage of the fuel cell and equals 0.7 V and q_{H_2} represents the amount of hydrogen which is consumed by the fuel cell (26.8 mol/h). Similarly, the input power limitation for the electrolyzer can be formulated as follows:

$$P_{wtpv-el}(t,s) \leq \frac{2 \times 2 \times 96487 \times n_{H_2}}{3600 \times 1000} \times N_{El} \qquad \mathbf{(4.31)}$$

where n_{H_2} is the amount of produced hydrogen by the electrolyzer (9.33 mol/h).

4.4 System Constraints

Besides component constraints, there are also constraints for the microgrid system such as area limitations and system power balance, etc. The system power balance equation can be shown as:

$$\begin{aligned} P^{+}_{Bat}(t,s) - P^{-}_{Bat}(t,s) + P^{+}_{EV}(t,s,c) - P^{-}_{EV}(t,s,c) + \ P_{Fc}(t,s) - \ P_{Wtpv-El}(t,s) \\ = P_d(t,s) - [P_{PV}(t,s) + P_{WT}(t,s)] - Dp(t,s) + Sp(t,s) \qquad \mathbf{(4.32)} \end{aligned}$$

where $Sp(t,s)$ denotes surplus production. The demand is divided into two parts non-critical and critical demand which is shown as:

$$P_d(t,s) = P_{d-c}(t,s) + P_{d-nc}(t,s) \qquad \mathbf{(4.33)}$$

$P_{d-c}(t,s)$ and $P_{d-nc}(t,s)$ represent the critical and non-critical demand respectively.

The LPSP was defined through the deficit power which should be less than or equal to the non-critical power as shown in (4.34) since the critical demand should be always compensated.

$$Dp(t,s) \le P_{d-nc}(t,s) \qquad \mathbf{(4.34)}$$

Finally, there is an area restriction where the microgrid system will be constructed which will affect the number of wind turbines and PV panels. This limitation can be shown as:

$$(A_{PV} \times N_{PV}) + (W_d \times W_{RS}) \times N_{WT} \le A_{MG} \qquad \mathbf{(4.35)}$$

where W_d represents wind turbine blade diameter, W_{RS} is the space required for a wind turbine and A_{MG} denotes the area which is available for the construction of the rural microgrid system.

Chapter 5

Results and Discussion

In this section, the data collection and the results will be presented.

5.1 Data Collection

In this thesis, hourly real-world data sets are utilized for a one-year period. The data for renewables which are wind speed (m/s) and solar irradiance (W/m^2) are taken from a firm named Fiba Energy and Solargis respectively. The data for renewables are for the same location Karaburun, İzmir/Turkey. The data sets are shown in Figures 3 and 4 respectively. The hourly demand data for one year is created by merging 14 residential data assuming there are 14 houses in the rural microgrid system. This data set is taken from Harvard Dataverse and shown in Figure 5.

Figure 3. Hourly wind speed.

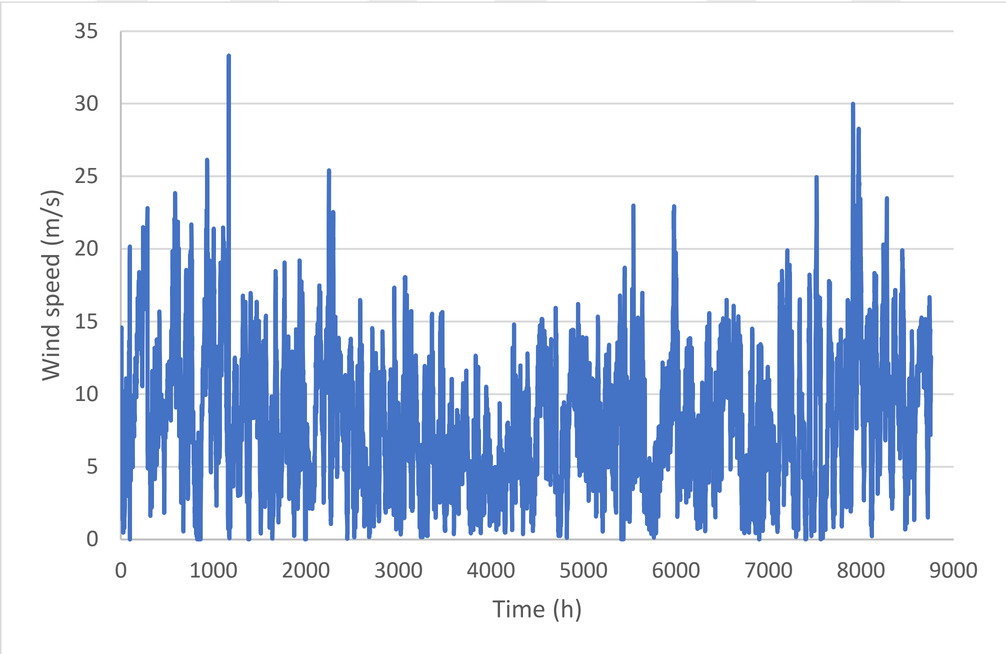

Figure 4. Hourly solar irradiance.

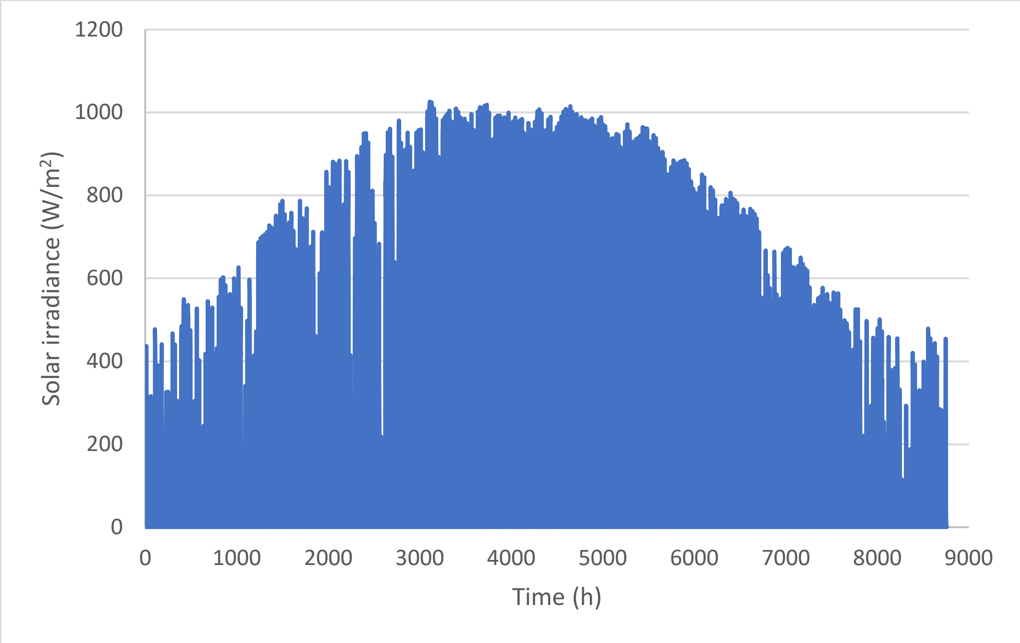

Figure 5. Hourly demand profile.

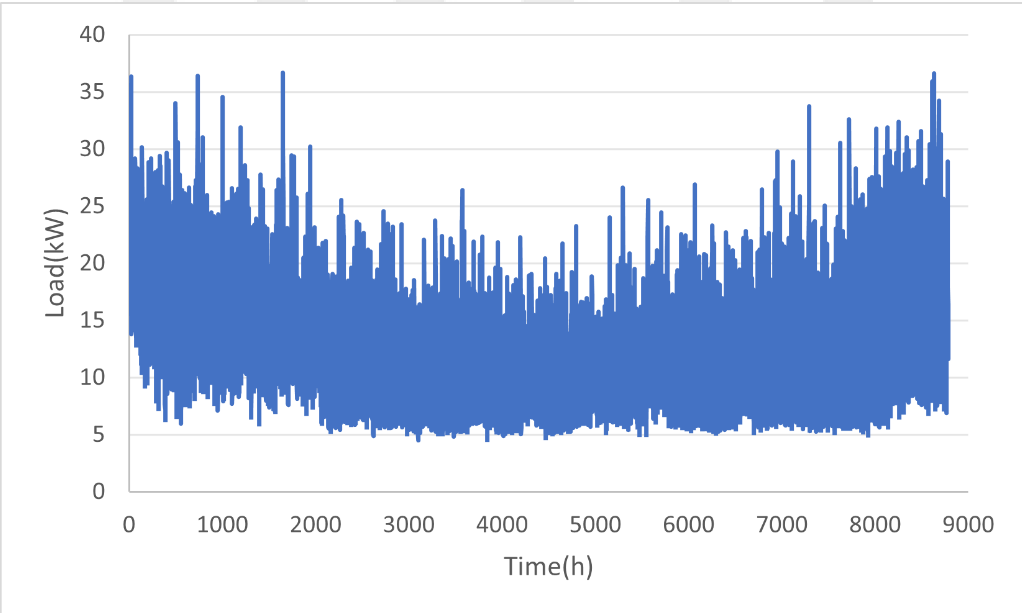

The EVs will be connected to the charging point when they arrive at the system. The charging will not be started directly, the time that the charging starts will be decided by the smart system. A 7.4 kW charger is used to charge electric vehicles. The arrival and departure times of EVs are defined separately for weekdays and weekends. The arrival time for weekdays is uniformly distributed between 18-22 and for weekends 17-23. The departure time for weekdays takes a value between 7-11 and for weekends 9-14. In addition, the SOC values of EVs during arrival and departure time is also defined in a specific range. The arrival SOC of EVs for weekdays and weekends is uniformly distributed between 20%-60% and the departure SOC should be 80% for the satisfaction of the EV owner.

The cost values and the lifetime of the components in the microgrid system are shown in Table 2. These parameters are taken from (Mohseni et al., 2020, pp. 114224), (Vahid et al., 2020, pp. 465-485), and (Adefarati et al., 2019, pp. 1089-1114).

Table 2: Cost and lifetime of the components.

Component	CC ($)	OC($/year)	RC ($)	Lifetime (years)
Wind turbine	3200/unit	32/unit	-	25
PV panel	2000/unit	20/unit	-	25
Battery	300/unit	10/unit	300/unit	5
Electrolyzer	800/kW	16/kW	-	25
Hydrogen tank	470/kg	1/kg	-	25
Fuel cell	2400/kW	120/kW	2400/kW	5

In Table 3, the other input parameters for components are shown. The parameters are taken from (Adefarati et al., 2019, pp. 1089-1114), (Moghaddam et al., 2019, pp. 1412-1434), and (Vahid et al., 2020, pp. 465-485). In addition, there are parameters related to the system in general. The interest rate i is 10%, the lifespan of the project is planned as 25 years and the total available construction area is limited to 10000 m^2.

Table 3: Other parameters of the components.

Component	Parameter
Wind turbine	Rated power = 1000 W v_{cut-in} = 3 m/s $v_{cut-out}$ = 25 m/s v_r = 11 m/s W_{RS} = 25 m^2 Swept area = 5.73 m^2 Diameter= 2.7 m^2
PV panel	Rated power = 1000 W n_{PV}= 15.5% Area = 1.95 m^2
Battery	Capacity = 4 kWh $SOC_{max-Bat}$ = 80% $SOC_{min-Bat}$ = 20% $P^{+}_{Bat-max}$ = 6910 W $P^{-}_{Bat-max}$ = 4610 W n^{+}_{Bat} = 90% n^{-}_{Bat} = 80%
Electrolyzer	n_{El} = 75%
Hydrogen tank	n_{Ht} = 95%
Fuel cell	n_{Fc} = 50%

There are ten EVs in the system, to be more realistic three different type of vehicles are utilized which have different efficiency levels and capacities. In Table 4, the parameters related to utilized car models are shown.

Table 4: The parameters of electric vehicle models.

Model	Charge & Discharge Efficiency	Capacity (kWh)	Number of the cars
BMW i3	92.2%	18.8	3
Nissan Leaf	86%	24	4
Renault Zoe	87%	41	3

In each case, the EV can be used as a storage device which will both supply energy and take energy from the microgrid system. The other option is EV will only take energy from the microgrid system which means it will act as a consumer. In order to clarify these roles Table 5 is created.

Table 5: The electric vehicle cases.

Case	Description	Storage Device (S)	Consumer (C)
EV	As in Table 5.2	EV-S	EV-C

For instance, in EV-S case, there will be three types of cars as shown in Table 4 and the cars will act as a storage device which means when there is a need, they will supply energy to the system if the car is in the system and it can also be charged from the system. On the other hand, in EV-C case, the vehicles will be only charged from the system, they will not supply energy to the system even if there is a need.

5.2 Results

In this thesis, the optimal sizing of a rural microgrid is studied. Gurobi Optimizer is utilized to simulate the optimization model by the Gurobi Python interface. According to the ε-constraint method, which is defined in Section 3.1, LPSP is used as ε-constraint. As a result, all scenarios are solved according to different LPSP limits (0, 0.1, 0.2). The LPSP limits show the maximum LPSP value, it does not mean that LPSP should be directly equal to that limit. In most scenarios, LPSP will be less than the specified LPSP limit, which will provide smaller deficiencies with higher system reliability.

There are mainly three cases which are created to analyze the impact of the storage types in the optimal system design. These cases are shown in Table 6.

Table 6: Description of the cases.

Case	Description
1	The number of batteries is limited with 100 units.
2	There is no limitation in the number of batteries.
3	There are no batteries in the system.

In the first model the hydrogen storage will be included by restricting the number of batteries as follows:

$$N_{Bat} \leq 100 \qquad (\mathbf{5.1}).$$

This constraint will cause a need for the hydrogen storage since the number of batteries will not be enough as a storage system. On the other hand, in the second model the equation (5.1) will be removed which means there will not be any limitation in the number of batteries. Because of the important difference between the cost values of batteries and the hydrogen storage, in this model hydrogen storage will not exist.

The simulations are completed for LPSP limits of 0, 0.1 and 0.2. The number/capacity of the components and cost values are shown in Table 7.

Table 7: The number/capacity of components and cost values with constraint (5.1).

	LPSP limit	Wind Turbine	PV	Battery	Electrolyzer *(W)*	Hydrogen tank *(kg)*	Fuel cell *(W)*	LCC ($)
EV-S	0	52	1455	64	0	0	0	802815.5
	0.1	55	1265	39	0	0	0	717903.1
	0.2	92	923	23	0	0	0	637563.7
EV-C	0	35	1573	100	6176.27	1719.92	3730.46	918456.7
	0.1	38	1377	91	0	0	0	738089.8
	0.2	38	1197	66	0	0	0	651254.4

It is seen from Table 7 that for both EV scenarios the increase in LPSP causes a drop in the LCC. The reason for this drop is the decrease in the number of components since reliability is decreasing. The number of wind turbines was not significantly affected when the LPSP level is changed and there is a visible drop in the number of PV panels and batteries. Another important result is related to hydrogen storage. Only in one case hydrogen storage is installed which is for the EV-C case where the vehicles consume energy from the system and LPSP equals 0. Because of the high cost values of the hydrogen storage components, the highest LCC is observed in this situation which is around $100000 higher than the EV-S case for the same LPSP level. Also, a decrease in the number of components and LCC can be observed when the role of EV is changed to EV-S. Since cars act as storage devices in this role, the need for other storage devices (battery/hydrogen storage) and generation units will decrease. On the other hand, in the second model constraint (5.1) is removed from the model. The result of this simulation is shown in Table 8.

Table 8: The number/capacity of components and cost values.

	LPSP limit	Wind Turbine	PV	Battery	LCC ($)
EV-S	0	52	1455	64	802815.5
	0.1	58	1251	39	717952.1
	0.2	92	923	23	637563.7
EV-C	0	39	1553	116	825254.8
	0.1	38	1377	91	738089.8
	0.2	38	1197	66	651254.4

According to Table 8, the only difference from the previous model occurs in the EV-C case with LPSP level 0. Since the number of batteries can be greater than 100, 116 batteries are installed. As a result of this, hydrogen storage is no longer needed in this case since the batteries are cheaper. Because of the high costs of hydrogen storage components, there is an important difference in the LCC when compared with the previous model which is around $100000. In other scenarios, there is no change in the number of components and cost values since the number of batteries was already less than 100 in the previous model. The LCC according to LPSP limits for EV-S and EV-C cases with the battery restriction (equation 5.1) is shown in Figure 6. LCC of EV-C and EV-S cases.

Figure 6. LCC of EV-C and EV-S cases.

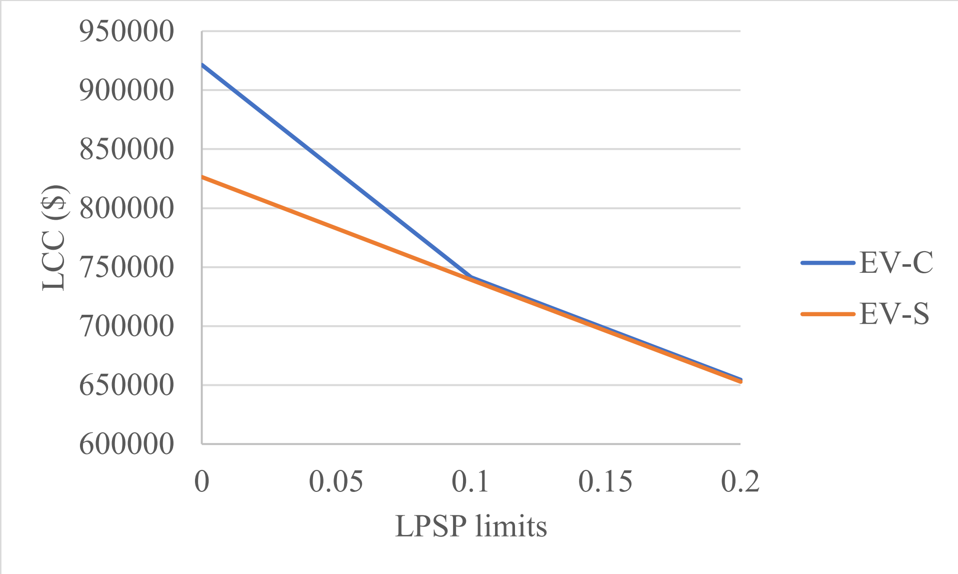

In another case, to analyze the impact in the number/capacity of system components and the cost values batteries is removed from the system as follows:

$$N_{Bat} \leq 0 \tag{5.3}$$

The simulation results after this limitation are shown in Table 9.

Table 9: The number/capacity of components and cost values with constraint (5.3).

	LPSP limit	Wind Turbine	PV	Electrolyzer *(W)*	Hydrogen tank *(kg)*	Fuel cell *(W)*	LCC ($)
EV-S	0	87	1513	78750.98	6863.822	30866.87	1294484
	0.1	114	1144	61245.49	4279.339	11349.84	1028116
	0.2	100	1010	52748.89	1555.614	4453.942	784638.6
EV-C	0	90	1987	104165	12575.57	36157.2	1831328
	0.1	102	1594	84052.17	9715.097	21580.7	1509543
	0.2	59	1485	74974.56	6941.483	15035.72	1211453

The results show that; after this restriction, the need for hydrogen storage increases significantly since it is the only storage alternative apart from EVs in the EV-S case. Since in EV-C cases hydrogen storage is the only storage option the capacity of each component is noticeably increased. If it is compared with the results in Table 8, the total LCC values are much higher as a result of the high costs of hydrogen storage components. In addition to this, the number of wind turbines is increased significantly in each case which also has an impact on the cost values. On the other hand, the number of PV panels is not significantly affected.

The average LPSP values of all scenarios according to LPSP limits are observed. These values are shown in Figure 7.

Figure 7. Average LPSP values.

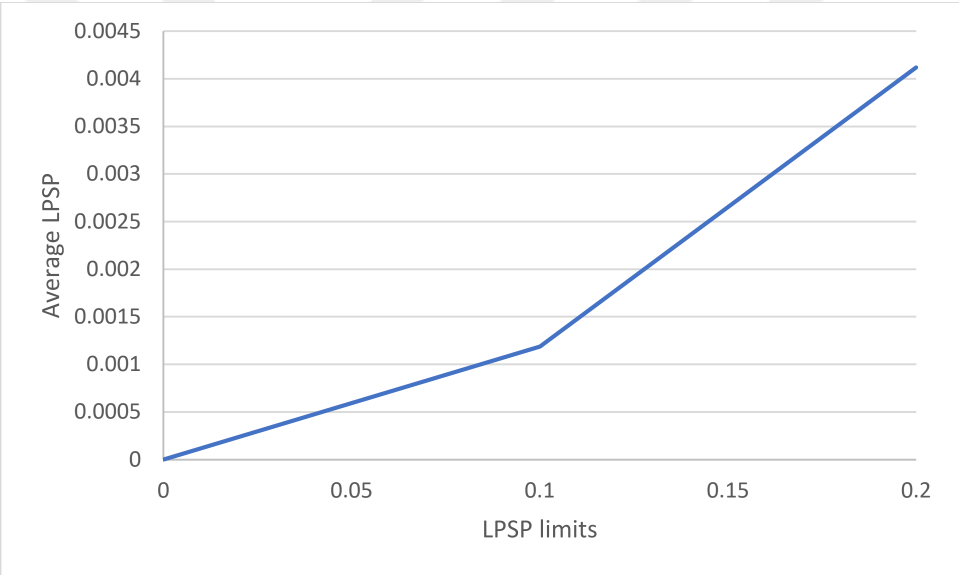

It is seen that average LPSP values do not exceed 0.0042 even in the highest LPSP limit 0.2. This means the system is approximately 99.5% reliable when LPSP limit is 0.2.

Chapter 6

Conclusion

In this thesis, the optimal sizing of a rural microgrid system is studied. The system consists of PV, wind turbine, battery, hydrogen storage (electrolyzer, hydrogen tank, fuel cell), and EV. Uncertainties from renewable generation, demand, and electrical vehicles are considered during modelling. To deal with the uncertainties in the system, two-stage stochastic optimization is applied. Real-world data is used for demand and renewables which are hourly data for one year.

The simulations show that the increase in LPSP value creates a drop in the number/capacity of components since the system becomes less reliable. This drop results in a lower LCC during system sizing. Another output of the study is related to the EV scenarios. Two roles of EV were simulated, if the EV acts as a storage system (EV-S) there is a decrease in the number of batteries and in the capacity of hydrogen storage components. Therefore, the total cost decreases significantly compared to the other role where the EVs are consumers (EV-C). In addition, when the number of batteries is restricted with 100 units, it is seen that there will be a need for hydrogen storage. This limitation is applied for environmental goals, even though hydrogen storage is more expensive. As a result of this limitation, in one scenario where EV is the consumer and LPSP equals zero, hydrogen storage is installed in the optimal design, and the other scenarios are not affected by this restriction since there were already less than 100 batteries. In the cases where the hydrogen storage is installed, there is a remarkable increase in the LCC because of the high cost of the components of the hydrogen storage. In addition to this, when batteries are removed from the system in each case a need for hydrogen storage arises. In EV-S scenarios this requirement is smaller since EVs are alternative storages and similar with the other cases in EV-C scenarios the required capacity for hydrogen storage is more which will end up with high cost values. Between three cases the highest cost values occur in the third case where batteries do not exist in the system design. Even if it results in an expensive design, hydrogen storage may replace the batteries in the future since it is environmentally friendly and sustainable.

REFERENCES

A. H. Fathima, K. Palanisamy, Optimization in microgrids with hybrid energy systems – a review, *Renewable and Sustainable Energy Reviews*, 45 (2015) 431–446.

Adefarati, T., & Bansal, R. C. (2019). Reliability, economic and environmental analysis of a microgrid system in the presence of renewable energy resources. *Applied energy*, *236*, 1089-1114.

Arun, P., Banerjee, R., & Bandyopadhyay, S. (2009). Optimum sizing of photovoltaic battery systems incorporating uncertainty through design space approach. *Solar Energy*, 83(7), 1013-1025.

B. S. Hartono, Y. Budiyanto and R. Setiabudy, "Review of microgrid technology," 2013 *International Conference on QiR*, 2013, pp. 127-132, doi: 10.1109/QiR.2013.6632550.

Balderrama, S., Lombardi, F., Riva, F., Canedo, W., Colombo, E., & Quoilin, S. (2019). A two-stage linear programming optimization framework for isolated hybrid microgrids in a rural context: The case study of the "El Espino" community. *Energy*, *188*, 116073.

Bashir, M. & Sadeh, J. (2012, May). Optimal sizing of hybrid wind/photovoltaic/battery considering the uncertainty of wind and photovoltaic power using Monte Carlo. In *2012 11th International Conference on Environment and Electrical Engineering* (pp. 1081-1086). IEEE.

F. S. Gazijahani, H. Hosseinzadeh, A. A. Abadi and J. Salehi, "Optimal day ahead power scheduling of microgrids considering demand and generation uncertainties," *2017 Iranian Conference on Electrical Engineering (ICEE)*, 2017, pp. 943-948, doi: 10.1109/IranianCEE.2017.7985174.

Fiba Energy, https://www.fibaenerji.com/en_US/home, 2022

G. C. Lazaroiu, V. Dumbrava, G. Balaban, M. Longo and D. Zaninelli, "Stochastic optimization of microgrids with renewable and storage energy systems," *2016 IEEE 16th International Conference on Environment and Electrical Engineering (EEEIC)*, 2016, pp. 1-5, doi: 10.1109/EEEIC.2016.7555486.

Gamarra C& Guerrero J.M. Computational optimization techniques applied to microgrids planning: A review, *Renew. Sustain. Energy Rev.*, 48 (2015), pp. 413-424

Gamil, M. M., Lotfy, M. E., Hemeida, A. M., Mandal, P., Takahashi, H., & Senjyu, T. (2021). Optimal sizing of a residential microgrid in Egypt under deterministic and stochastic conditions with PV/WG/Biomass Energy integration. *Aims Energy*, *9*(3), 483-515.

Gazijahani, F. S., & Salehi, J. (2018). Reliability constrained two-stage optimization of multiple renewable-based microgrids incorporating critical energy peak pricing demand response program using robust optimization approach. *Energy*, 161, 999-1015.

Guo, L., Liu, W., Jiao, B., Hong, B., & Wang, C. (2014). Multi-objective stochastic optimal planning method for stand-alone microgrid system. *IET Generation, Transmission & Distribution*, *8*(7), 1263-1273.

Gurobi Optimizer, https://www.gurobi.com/products/gurobi-optimizer/, 2022

Haidar, A. M., Fakhar, A., & Helwig, A. (2020). Sustainable energy planning for cost minimization of autonomous hybrid microgrid using combined multi-objective optimization algorithm. *Sustainable Cities and Society*, *62*, 102391.

Harvard Dataverse, https://dataverse.harvard.edu/dataset.xhtml?persistentId=doi:10.7910/DVN/N3HGRN, 2020.

Jacob A.S., Banerjee R., Ghosh P.C. (2021) Incorporating Battery Degradation in Stand-alone PV Microgrid with Hybrid Energy Storage. In: Bose M., Modi A. (eds) Proceedings of the 7th International Conference on Advances in Energy Research. *Springer Proceedings in Energy. Springer, Singapore*. https://doi.org/10.1007/978-981-15-5955-6_43

Kamjoo, A., Maheri, A., Dizqah, A. M., & Putrus, G. A. (2016). Multi-objective design under uncertainties of hybrid renewable energy system using NSGA-II and chance constrained programming. *International journal of electrical power & energy systems*, *74*, 187-194.

Kaviani, A. K., Riahy, G. H., & Kouhsari, S. M. (2009). Optimal design of a reliable hydrogen-based stand-alone wind/PV generating system, considering component outages. *Renewable energy*, *34*(11), 2380-2390.

Khiareddine, A., Salah, C. B., Rekioua, D., & Mimouni, M. F. (2018). Sizing methodology for hybrid photovoltaic/wind/hydrogen/battery integrated to energy management strategy for pumping system. *Energy*, *153*, 743-762.

M. A. Abdulgalil, M. N. Khater, M. Khalid and F. Alisamail, "Sizing of energy storage systems to enhance microgrid reliability," 2018 *IEEE International Conference on Industrial Technology (ICIT)*, 2018, pp. 1302-1307, doi: 10.1109/ICIT.2018.8352366.

Maheri, A. (2014). Multi-objective design optimisation of standalone hybrid wind-PV-diesel systems under uncertainties. *Renewable Energy*, *66*, 650-661.

Marler, R. T. (2005). *A study of multi-objective optimization methods for engineering applications*. The University of Iowa.

Moghaddam, M. J. H., Kalam, A., Nowdeh, S. A., Ahmadi, A., Babanezhad, M., & Saha, S. (2019). Optimal sizing and energy management of stand-alone hybrid photovoltaic/wind system based on hydrogen storage considering LOEE and LOLE reliability indices using flower pollination algorithm. *Renewable energy*, *135*, 1412-1434.

Mohseni, S., Brent, A. C., & Burmester, D. (2020). A comparison of metaheuristics for the optimal capacity planning of an isolated, battery-less, hydrogen-based micro-grid. *Applied Energy*, *259*, 114224.

Naderi, E., Dejamkhooy, A., Seyedshenava, S. J., & Shayeghi, H. (2022). MILP based Optimal Design of Hybrid Microgrid by Considering Statistical Wind Estimation and Demand Response. *Journal of Operation and Automation in Power Engineering*, *10*(1), 54-65.

Narayan, A., & Ponnambalam, K. (2017). Risk-averse stochastic programming approach for microgrid planning under uncertainty. *Renewable Energy*, *101*, 399-408.

Nazari, A., & Keypour, R. (2019). A two-stage stochastic model for energy storage planning in a microgrid incorporating bilateral contracts and demand response program. *Journal of Energy Storage*, 21, 281-294.

S. R. Bull, "Renewable energy today and tomorrow," *in Proceedings of the IEEE*, vol. 89, no. 8, pp. 1216-1226, Aug. 2001, doi: 10.1109/5.940290.

Sadeghi, D., Naghshbandy, A. H., & Bahramara, S. (2020). Optimal sizing of hybrid renewable energy systems in presence of electric vehicles using multi-objective particle swarm optimization. *Energy*, *209*, 118471.

Shadkam, E., & Jahani, N. (2015). A hybrid COA $\epsilon $-constraint method for solving multi-objective problems. *arXiv preprint arXiv:1509.08302*.

Solargis, https://solargis.com/, 2022

Stevanato, N., Lombardi, F., Guidicini, G., Rinaldi, L., Balderrama, S. L., Pavičević, M., ... & Colombo, E. (2020). Long-term sizing of rural microgrids: Accounting for load evolution through multi-step investment plan and stochastic optimization. *Energy for Sustainable Development*, *58*, 16-29.

Vahid, M. Z., hajivand, M., Moshkelgosha, M., Parsa, N., & Mansoori, H. (2020). Optimal, reliable and economic designing of renewable energy photovoltaic/wind system considering different storage technology using intelligent improved salp swarm optimisation algorithm, commercial application for Iran country. *International Journal of Sustainable Energy*, *39*(5), 465-485.